Research and Science Today
WWW.RSTJOURNAL.COM

DOI:

Title:	AERODYNAMIC ANALYSIS OF SIKORSKY UH-60 ROTARY WINGS
Authors:	Andrei GOGA

Section: ENGINEERING

Issue: 1(19)/2020

Received: 10 January 2020	**Revised:** 27 January 2020
Accepted: 9 March 2020	**Available Online:** 15 March 2020

RST Research and Science Today
WWW.RSTJOURNAL.COM
SPRING 2020
No. 1(19)/2020
ISSN-P: 2247-4455 / ISSN-E: 2285-9632

Engineering

AERODYNAMIC ANALYSIS OF SIKORSKY UH-60 ROTARY WINGS

Andrei GOGA[1]

ABSTRACT:
MODERN HELICOPTERS HAVE SEEN A SUBSTANTIAL IMPROVEMENT OVER THE YEARS. MISSIONS OF ALL TYPES WERE ASSIGNED AND THE NECESSITY OF HELICOPTERS RAISED, SO THOSE NEED TO BE AS PERFORMANT AS IT CAN. THE SIKORSKY UH-60 BLACK HAWK IS A VERY GOOD EXAMPLE OF MULTIROLE HELICOPTER USED BY A LOT OF COUNTRIES ALL OVER THE WORLD. THIS PAPER ILLUSTRATES 3D SIMULATIONS OF SEVERAL VARIANTS FOR THE MAIN ROTOR BLADES BY EXPOSING PERFORMANCE ANALYSIS USING A SOFTWARE TOOL ON AN EQUIVALENT MODEL.

KEY WORDS: BLACK HAWK, UH-60, QBLADE, HELICOPTER, PERFORMANCE

Simbols and acronyms

V	*Speed (m/s)*	*h*	*Air column above the blade (m)*
AFB	*Air Force Base*	NACA	*The National Advisory Committee for Aeronautics*
AEFA	*Aviation Engineering Flight Activity*	TSR	*Tip speed ratio*
BIMt	*Blade inspection method*		

1. INTRODUCTION

Wind tunnel testing has been extensively used in the development and improvement of rotorcraft designs in addition to providing databases for refinement of theoretical models. The Sikorsky UH-60 helicopter is one of the more thoroughly tested rotorcraft systems, having undergone extensive flight and model-scale wind tunnel testing. One of those testing has included hover and forward flight performance tests conducted by the U.S. Army Aviation Engineering Flight Activity (AEFA) at Edwards AFB and tests of a highly-instrumented rotor [2] at the U.S. Army Aeroflightdynamics Directorate and NASA Ames Research Center.

To expand the existing UH-60 database and to investigate rotor performance and loads in the low speed flight regime, a full-scale UH-60 rotor test has been conducted in the 80 x 120m wind tunnel. In this paper is shown a theoretical analysis of model blades,

[1] "Henri Coanda" Air Force Academy, Brasov
[2]Technical manual UH-60; DEPARTMENT OF THE ARMY 31 OCTOBER 1996 available at http://www.dtic.mil/dtic/tr/fulltext/u2/a409934.pdf

designed using 2D and 3D software, to extent the database of UH-60 and give some information about the influence of the design and its limitations.

Sikorsky UH-60 helicopter

2.GENERAL CONSIDERATIONS REGARDING SIKORSKY UH-60 MAIN ROTOR

The UH-60 main rotor system consists of four subsystems: main rotor blades, hub, flight controls and the vibration absorber. Four titanium-spar main rotor blades attach to spindles which are retained by elastomeric bearings contained in one-piece titanium hub. The elastomeric bearing permits the blade to flap, lead and lag. Lag motion is controlled by hydraulic dampers and blade pitch is controlled through adjustable control rods which are moved by the swash plate.

When the rotor is not turning, the blades and spindles rest on hub mounted droop stops. Upper restraints called anti-flapping stops retain flapping motion caused by the wind. Both stops engage as the rotor slows down during engine shutdown. Blade retaining pins can be pulled from the blade spindle joint and the blades folded along the rear of the fuselage [3].

The vibration absorber reduces rotor vibration at the rotor. The absorber is mounted on top of the hub and consists of a four arm plate with attached weights. Main rotor dampers are installed between each of the main rotor spindles modules and the hub to restrain hunting (lead and lag motions) of the main rotor blades during rotation and to absorb rotor head starting loads.

2.1 UH-60 main rotor blades

The structure aft of the spar consists of fiberglass skin, Nomex honeycomb filler and a graphite/fiberglass trailing edge. The leading edge of each blade has a titanium abrasion strip, the outboard portion of which is protected by a replaceable nickel strip. Electro-thermal blankets are bonded into the blades leading edge for deicing. A Blade Inspection Method (BIMt) indicator is installed on each blade at the root end trailing edge to visually indicate when blade spar structural integrity is degraded. If a spar crack occurs, or a seal leaks, nitrogen will escape from the spar. When the pressure drops below minimum the indicator will show red bands. A manual test lever is installed on each BIM indicator to provide a maintenance check.

[3] Thomas R. Norman "Full-Scale Wind Tunnel Test of the UH-60A Airloads Rotor" available at https://rotorcraft.arc.nasa.gov/Publications/files/AHS11_TestSummary_Norman.pdf

The blades are attached to the rotor head by two quick-release expandable pins[4], that require no tools to either remove or install. To conserve space, all blades can be folded to the rear and downward along the tail cone.

Table 1. Main rotor specifications

Rotor diameter	16.36m	Max. RPM	258
Disc area	210m^2	Airfoils	SC1095 / SC1095R8

3. SOFTWARE ANALYSIS

3.1 Software description

QBlade is an open source wind turbine simulation and calculation software hosted by sourceforge.net. The integration of the XFOIL/XFLR5 functionality allows the user to design airfoils and analyze them in 2D and 3D (lifting surface) [5,6]. The software is adequate for teaching, as it provides an easy way to simulate a model wind turbine.

QBlade also provides processing functionality for the rotor and turbine. In addition to that, the software is a very flexible and user-friendly platform for wind turbine blade design that can be used to simulate rotary wings for educational purposes.

XLFR5 is an airfoil design and analysis program, the most "user-friendly" of its type. This software uses the vortex panel method and integral boundary layer equations to calculate airfoil pitching moment at different angles of attack, drag and lift. Direct comparisons of up to three airfoils at a time may be performed. Changes to the performance characteristics of an airfoil may be made in seconds. The airfoil can be defined using NACA feature or introducing the specific coordinates. Results show an excellent comparison to published wind tunnel data [7].

3.2 Airfoils analysis

The SC1095 airfoil and the SC1095 R8 airfoil, modified from the SC1095 by adding droop at the leading edge, are illustrated in figure 1. The effect of the nose droop was to extend the SC1095 chord from 20.76 in. to 20.965 in., thereby reducing the airfoil thickness from 9.5 percent to 9.4 percent. The addition of nose droop also rotated the mean chordline by –1°, as shown in figure 1.

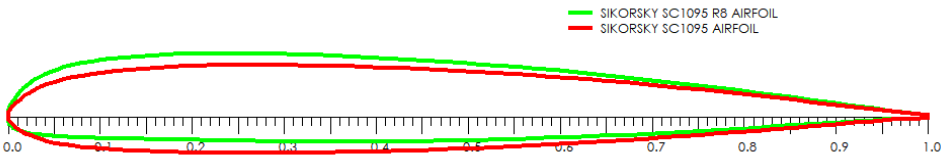

Figure 1. SC1095(red) and SC1095R8(green)

Table 2 Simulation parameters

Air density	1.225 (kg/m^3)	Reynolds number	8,250,000
Relax factor	0.35	Velocity	221m/s (tip speed)
Viscosity	1.465(mPa·s)		

[4] Helicopter Flying Handbook Version 1/2009 https://www.faa.gov/regulations_policies/handbooks_manuals/aviation/helicopter_flying_handbook/media/hfh_ch11.pdf
[5] Vasile Prisacariu THE AERODYNAMIC ANALYSIS OF HIGH LIFT DEVICES
[6] QBlade open-source software hosted by https://q-blade.org
[7] XFLR5 Guidelines hosted by http://www.xflr5.tech/xflr5.htm

The lift coefficient of a fixed-wing aircraft varies with angle of attack. Increasing angle of attack is associated with increasing lift coefficient up to the maximum lift coefficient, after which lift coefficient decreases. A symmetrical wing has zero lift at 0 degrees angle of attack. The lift curve is also influenced by the wing shape, including its airfoil section and wing plan form. A swept wing has a lower, flutter curve with a higher critical angle. For SC1095 the highest value of lift coefficient (1.86) corresponds with an angle of 18.6 and for SC1095R8 the lower value of lift coefficient (1.55) corresponds with an angle of 13.5° (see fig.2).

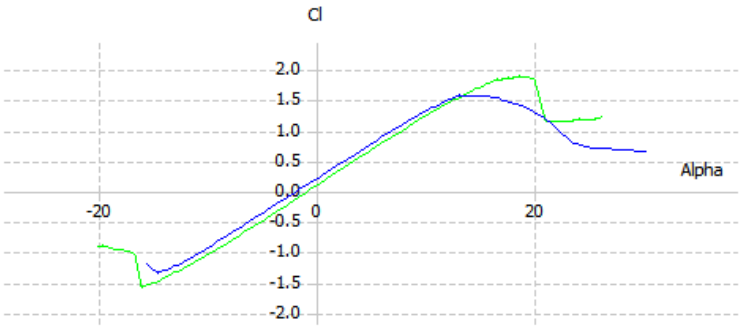

Fig. 2 Lift coefficient values between -20° and 30° for SC1095(green) and SC1095R8 (blue)

In aviation, induced drag tends to be greater at lower speeds because a high angle of attack is required to maintain lift, creating more drag (see fig.3) [8]. However, as speed increases the angle of attack can be reduced and the induced drag decreases. Parasitic drag, however, increases because the fluid is flowing more quickly around protruding objects increasing friction or drag. For SC1095 airfoil, the smallest value of drag coefficient is $5.7*10^{-3}$ at an angle of attack of 3.2° and for SC1095R8, the value of minimum is 5.55 at an angle of attack of 3.3°.

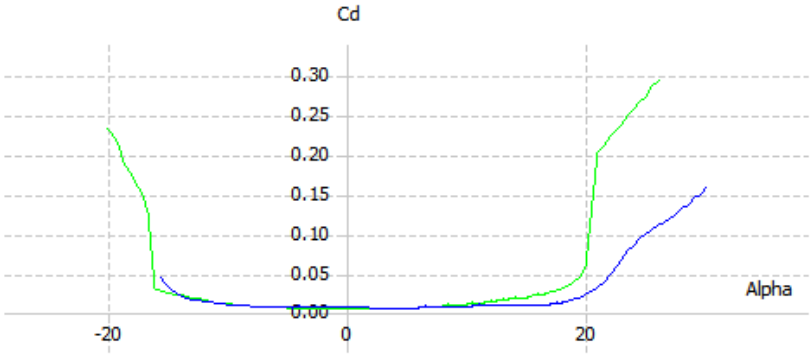

Fig. 3 Drag coefficient between -20° and 30° for SC1095(green) and SC1095R8 (blue)

Line missing - the airfoil could not be converged.

The glide ratio (see fig.4) is numerically equal to the lift-to-drag ratio, but is not necessarily equal during maneuvers, especially if speed is not constant. A glider's glide ratio varies with airspeed, but there is a maximum value which is frequently quoted. Glide ratio

[8] John D Anderson Jr.(2007) Fundamentals of aerodynamics, Fourth Edition ISBN 007-1254-08-0

usually varies little with vehicle loading [9]; a heavier vehicle glides faster, but nearly maintains its glide ratio.

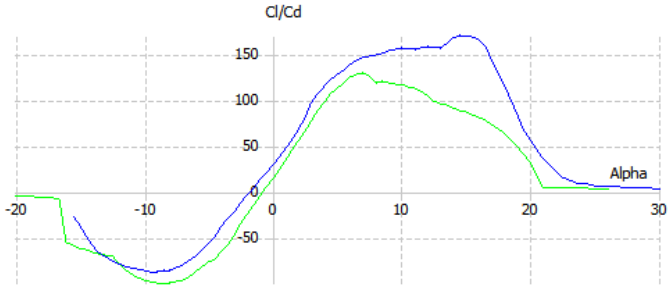

Fig. 4 Glide ratio for SC1095 and SC1095R8 airfoils for SC1095(green) and SC1095R8 (blue)

In fluid dynamics, a stall is a reduction in the lift coefficient generated by a foil as angle of attack increases. This occurs when the critical angle of attack of the foil is exceeded [10]. The critical angle of attack is typically about 15 degrees, but it may vary significantly depending on the fluid, foil, and Reynolds number.

The graph shows that the greatest amount of lift is produced as the critical angle of attack is reached. This angle is 18.6 degrees in SC1095 airfoil case, but it varies from airfoil to airfoil. In particular, for aerodynamically thick airfoils, the critical angle is higher than with a thin airfoil of the same camber. Symmetric airfoils have lower critical angles. The graph shows that, as the angle of attack exceeds the critical angle, the lift produced by the airfoil decreases (see fig 5).

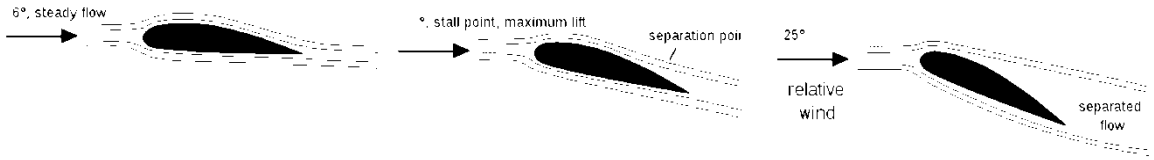

Fig. 5 Stall point illustration

3.3 Blades 3D analysis

A propeller creates a thrust force out of the supplied power [11]. The magnitude of this force is not constant for a given propeller, but depends on the velocity of the incoming air and the rotational velocity of the propeller itself. Thus tests of propellers usually cover a wide regime of operating conditions.

Table 3 Simulation parameters

Air rho	1.225 kg/m^3	Tip Speed Ratio	1…20
Relax factor	0.35	Velocity	221m/s
Viscosity	1.465 mPa·s		

[9] John D Anderson Jr.(2007) Fundamentals of aerodynamics, Fourth Edition ISBN 007-1254-08-0
[10] Principles of Flight, 2-18 and 3-1, Nordian Aviation Training Systems, 2017, ISBN 828107148
[11] Design and Analysis of Black Hawk UH-60 Rotor Blade Using Composite Materials;Dr. M Satyanarayana Gupta,Mr Badugu Uday Kumar ;September 2016
http://www.ijmetmr.com/olseptember2016/BaduguUdayKumar-MSatyanarayanaGupta-105.pdf

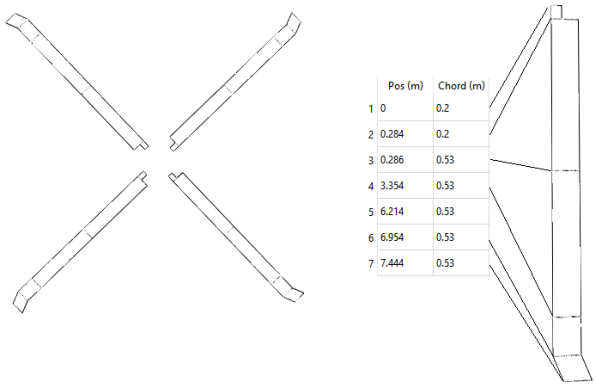

Fig 6 UH-60 Rotor blades with positions and chord lengths

The area under the graph illustrates the efficiency of the propeller(see fig. 7)

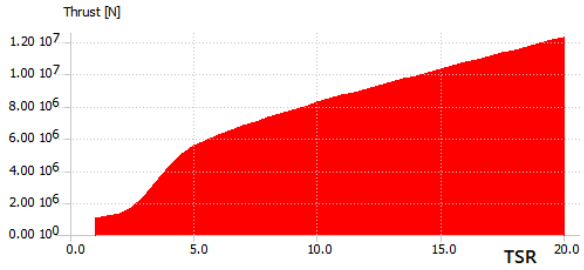

Fig. 7 Rotor efficiency

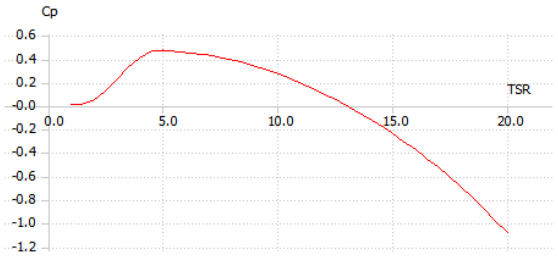

Fig. 8 The curve of power for UH-60 rotor

The relationship between the wind speed and the rate of rotation of the rotor in characterized by a non-dimensional factor known as Tip speed ratio TSR [12]. Power coefficient as a function of the TSR for a four bladed rotor determines the curve of power(see fig.8). Maximum power occurs at the optimal TSR.

Maximum airflow trough the main rotor:

$Volume = h \cdot \left(\pi R^2 - \pi r^2\right)$, *for one blade, one rotation*

$h = \sin(18.6) \cdot C$

$h = 0.3189 \cdot 0.53 = 0.169m = 16.9cm$

$V = 0.169(\pi \cdot 8.18 - \pi \cdot 0.736) = 395.2$

$AirFlow = V \cdot bl\_n \cdot RPM$

$AirFlow = 395.2 \cdot 4 \cdot 258$

$AirFlow = 407846 m^3 / \min$

[12] David Marten, Juliane Wendler, Qblade Guidelines, 2013, 76 , available at http://q-blade.org/project_images/files/guidelines_v06.pdf

ISSN-P: 2247-4455 / ISSN-E: 2285-9632

3.4 Modified blades analysis

3.4.1. Longer blades (+0.5m)

Helicopter longer blades solution is a highly reliable one for improving the lifting force. However, the lateral and longitudinal stability may be affected by the modifications, because of the higher centrifugal and centripetal forces acting on the blades in flight.

Simulation parameters are the same one as the first analysis.

Consequences of longer blades:

Airflow: from 407846m^3/min to 435194m^3/min

- *higher Maximum Takeoff Weight apx 25000lbs*
- *higher Maximum Speed apx 170Kts*
- *higher Service Ceiling apx 20250ft*
- *higher fuel consumption*

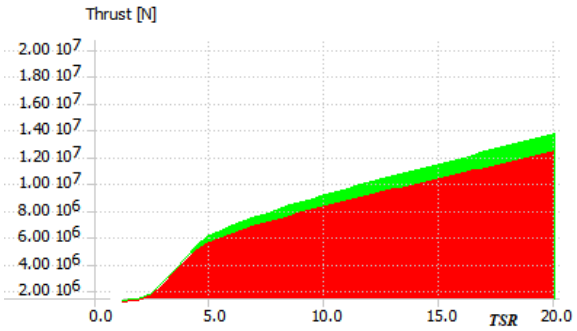

Fig. 9 Original rotor vs longer blades rotor efficiency

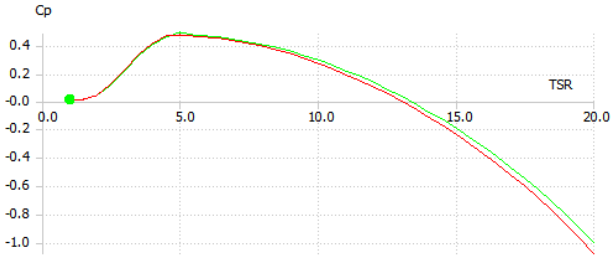

Fig 10 Power curves-original (red) vs. longer blades rotors (green)

The efficiency of the main rotor is characterized by the relation between the thrust and the tip speed ratio of that blades [13]. Yet, the efficiency of the main rotor is the area under the graph; red for the original rotor and green for the rotor with longer blades, which you can see it has a 8-9 % improvement.

The power curve in figure 10 illustrates that the highest point is about the same for the configurations, but also it can be seen that the longer blades rotor requires a little bit more power to work.

3.4.2 Wider blades (+0.1m)

Simulation parameters are the same one as the first analysis.

Consequences of wider blades

Airflow: from 407846m^3/min to 517651m^3/min

- *higher Maximum Takeoff Weight apx 30000lbs*
- *higher Maximum Speed apx 200Kts*
- *higher Service Ceiling apx 24000ft*
- *higher fuel consumption*

[13] Prisacariu V., *CFD Analysis of UAV Flying Wing*, INCAS Bulletin, vol. 8, 3/2016, ISSN 2066 – 8201, DOI: 10.13111/2066-8201.2016.8.3.6, p 65-72

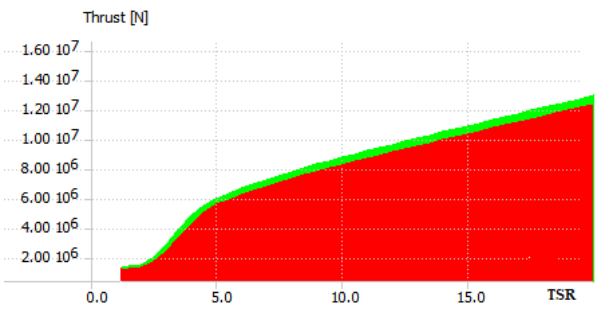

Fig. 11 Original rotor vs wider blades rotor efficiency

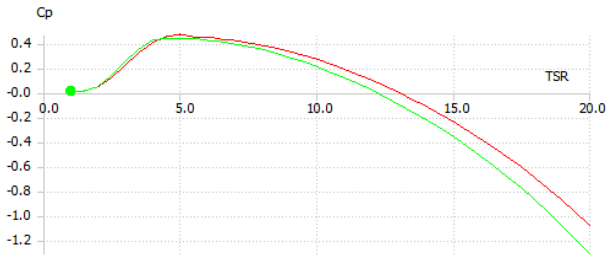

Fig 12. Power curves-original (red) vs longer blades rotors(green)

The efficiency of the main rotor is characterized by the relation between the thrust and the tip speed ratio of that blades. Yet, the efficiency of the main rotor is the area under the graph; red for the original rotor and green for the rotor with wider blades, which you can see it has a 3-4 % improvement[14].

The power curve in figure 12 illustrates that the highest point[15] is about the same for the configurations, but also it can be seen that the wider blades rotor requires a little bit more power to work.

Author conclusions regarding the theme

1. The effect of the dimensions for blades; wider and longer blades mean higher lift and efficiency, but for this to happen there must be considered a more powerful engine or a higher fuel consumption
2. The airfoil must prefferably be wider to delay the separation of the limit layer.

Author contributions regarding the theme

1. Determining the influence of blades dimensions for a modern helicopter
2. Analyse and illustrate SC1095 and 1095R8 airfoils properties and limitations
3. Execute a 1:1 model of the rotors using the same airfoils as the manufacturer did.

[14] The aerodynamic analysis of the profiles for flying wings, JOURNAL OF DEFENSE RESOURCES MANAGEMENT, vol.4 issue 1(6)/2013, ISSN:2068-9403, eISSN:2247-6466, ISSN-L: 2247-6466, p211-218

[15] Prisacariu V., Boşcoianu C., Luchian A., Considerations of the bird strike on aircraft wing, RECENT Journal, Vol. 18, no. 2(52), July, 2017, Transilvania University of Brasov, Romania, ISSN 1582-0246, p 109-115

ISSN-P: 2247-4455 / ISSN-E: 2285-9632

REFERENCES

1. Technical manual UH-60; DEPARTMENT OF THE ARMY 31 OCTOBER 1996 available at http://www.dtic.mil/dtic/tr/fulltext/u2/a409934.pdf
2. **Thomas R. Norman** "Full-Scale Wind Tunnel Test of the UH-60A Airloads Rotor" available at https://rotorcraft.arc.nasa.gov/Publications/files/ AHS11_TestSummary_Norman.pdf
3. Helicopter Flying Handbook Version 1/2009 https://www.faa.gov/regulations_policies /handbooks_manuals/aviation/helicopter_flying_handbook/media/hfh_ch11.pdf
4. **Prisacariu, Vasile; Chirilă, Alexandru**; Aerodinamic analysis of helicopter fenestron vertical tail, Scientific research and education in the Air Force– AFASES 2019, ISSN, ISSN-L : 2247-3173, p176-183, DOI: 10.19062/2247-3173.2019.21.24
5. **David Marten**, Qblade Short Manual, available at https://www.researchgate.net/publication
6. /281279669_QBlade_Short_Manual_v08;
7. XFLR5 Guidelines, hosted by http://www.xflr5.tech/xflr5.htm
8. **M Satyanarayana Gupta, Badugu Uday Kumar**, Design and Analysis of Black Hawk UH-60 Rotor Blade Using Composite Material, September 2016, available at http://www.ijmetmr.com/ olseptember2016/BaduguUdayKumar-MSatyanarayanaGupta-105.pdf
9. **Prisacariu, Vasile**; Aerodynamic analysis of UAVs. MFD Nimbus, nr. 2(11)/2019, INCAS Bulletin, (P) ISSN 2066-8201, (E) ISSN 2247-4528, DOI: 10.13111/2066-8201.2019.11.2.11, p.135-145
10. Principles of Flight, 2-18 and 3-1, Nordian Aviation Training Systems, 2017, ISBN 8281071486,
11. 9788281071483,
12. **Prisacariu,Vasile**; The aerodynamic analysis of the profiles for flying wings, JOURNAL OF DEFENSE
13. RESOURCES MANAGEMENT, vol.4 issue 1(6)/2013, ISSN:2068-9403, eISSN:2247-6466, ISSN-L:
14. 2247-6466, p211-218.
15. **David Marten, Juliane Wendler**, Qblade Guidelines, 2013, 76p. , available at http://qblade.org/project_images/files/guidelines_v06.pdf
16. **John D Anderson Jr.(2007)** Fundamentals of aerodynamics, Fourth Edition ISBN 007-1254-08-0;